

# On nonlocal mechanics of curved elastic beams

Preprint of the article published in  
International Journal of Engineering Science  
144, November 2019, 103140

Raffaele Barretta,  
Francesco Marotti de Sciarra,  
Marzia Sara Vaccaro

<https://doi.org/10.1016/j.ijengsci.2019.103140>

© 2019. This manuscript version is made available under the CC-BY-NC-ND 4.0 license <http://creativecommons.org/licenses/by-nc-nd/4.0/>

# On nonlocal mechanics of curved elastic beams

Raffaele Barretta<sup>a</sup>, Francesco Marotti de Sciarra<sup>a</sup>, Marzia Sara Vaccaro<sup>a</sup>

<sup>a</sup> *Department of Structures for Engineering and Architecture,  
University of Naples Federico II, via Claudio 21, 80125 - Naples, Italy  
e-mails: rabarret@unina.it - marotti@unina.it - marziasara.vaccaro@unina.it*

---

## Abstract

Curved beams are basic structural components of Nano-Electro-Mechanical-Systems (NEMS) whose design requires appropriate modelling of scale effects. In the present paper, the size-dependent static behaviour of curved elastic nano-beams is investigated by stress-driven nonlocal continuum mechanics. Axial strain and flexural curvature fields are integral convolutions between equilibrated axial force and bending moment fields and an averaging kernel. The nonlocal integral methodology formulated here is the generalization to curved structures of the treatment in [Int. J. Eng. Science 115 (2017) 14-27] confined to straight beams. The corresponding nonlocal differential problem, supplemented with non-standard boundary conditions, is highlighted and shown to lead to mathematically well-posed problems of nano-engineering. The theoretical predictions, exhibiting stiffening nonlocal behaviours, are therefore appropriate to significantly model a wide range of small-scale devices of nanotechnological interest. The nonlocal approach is exploited by analytically establishing size-dependent responses of curved elastic nano-sensors and nano-actuators that are driven by the small-scale characteristic parameter.

*Key words:* Curved beams, Size effects, Integral elasticity, Stress-driven nonlocal model, Nanotechnology, MEMS/NEMS

---

## 1. Introduction

Analysis, modelling, design, optimization and realization of smaller and smaller structural devices is nowadays a topic of major interest in Engineering Science, due to the recent advancements in Nanoscience and Nanotechnology.

A large number of contributions have been published on size-dependent structural behaviour of rods, wires, beams, membranes, plates and shells at micro- and nano-scales to conceive modern small-scale systems, such as: varactors (Sedighi et al., 2017), energy harvesters (Lekha et al., 2017), piezoelectric devices for biomedicine applications (Salim et al., 2018), resonators (Chorsi and Chorsi, 2018), resonant accelerometers (Ding et al., 2019), biosensors for detection of malaria protozoan parasites (Kurmendra et al., 2019) and of cancer (Kurmendra et al., 2019), arch actuators (Ouakad and Sedighi, 2019). In this context, curved beams are the main structural elements of Micro/Nano-Electro-Mechanical-Systems (M/NEMS) resonators (Dantas and Gusso, 2018; Alfosail et al., 2019; Frangi and Gobat, 2019; Nikpourian et al., 2019; Ouakad and Najjar, 2019; Sieberer et al., 2019; Wang and Ren, 2019) that should be designed by significantly taking small size effects into account. Only a few papers have been published on the matter and, however, scale phenomena have been modelled by strain-driven nonlocal or couple stress methods, which, as discussed below, present some operational difficulties.

1. **Eringen differential nonlocal model.** Such a strategy, recently employed in (Ganapathi and Polit, 2017; Aya and Tufekci, 2017; Polit et al., 2018; Rezaiee-Pajand and Rajabzadeh-Safaei, 2018; Arefi et al., 2019), is based on the differential relation associated with the strain-driven fully nonlocal integral convolution of the theory of elasticity, originally exploited by Eringen (1983) to tackle small-scale problems, defined in unbounded domains, of screw dislocation and wave propagation. Such a model has been shown to provide, in the special case of straight structures, mechanical paradoxes (Peddieson et al., 2003; Challamel and Wang, 2008; Li et al., 2015; Fernández-Sáez et al., 2016) and size-dependent responses which are of limited applicative interest. Inapplicability of Eringen's strain-driven fully nonlocal integral model of elasticity to nanostructures has been highlighted by Romano and Barretta (2016); Romano et al. (2017) and, nowadays, acknowledged by the scientific community of Engineering Science. As a partial remedy, Eringen's strain-driven fully nonlocal integral model has been replaced with the strain-driven local/nonlocal mixture (Eringen, 1972, 1987) to capture size effects (Wang et al., 2016; Fernández-Sáez and Zaera, 2017; Zhu et al., 2017; Khaniki, 2019; Zhang et al., 2019), even if it exhibits singular structural behaviors for vanishing local fractions (Romano et al., 2017).

2. **Nonlocal strain gradient model.** This strategy, based on the differential law associated with the strain-driven nonlocal strain gradient integral model, was originally conceived by [Lim et al. \(2015\)](#) for applications in wave propagation. In curved structures, the non-standard constitutive boundary conditions associated with the nonlocal gradient integral convolutions have been ignored ([She et al., 2019a,b](#); [Karami et al., 2019b](#); [Sobhy and Abazid, 2019](#); [Ebrahimi and Barati, 2018, 2017](#)) and non-pertinent higher-order boundary conditions of strain gradient theory have been enforced. This issue has been recently addressed by [Barretta and Marotti de Sciarra \(2018, 2019\)](#) for straight nanobeams, and advantageously exploited by [Apuzzo et al. \(2018, 2019\)](#).
3. **Modified couple stress model.** Such a strategy, proposed by [Yang et al. \(2002\)](#), has been widely applied to small-scale structures (see e.g. [Dehrouyeh-Semnani et al., 2017a,b](#); [Farokhi et al., 2017](#); [Ghayesh and Farokhi, 2017a,b](#); [Farokhi and Ghayesh, 2018a,b,c](#); [Ghayesh et al., 2018](#); [Khorshidi, 2018](#); [Taati, 2018](#); [Ghayesh, 2019](#); [Karami et al., 2019a](#)). Nevertheless, deformation measures describing couple stress theories are kinematically redundant, as evidenced by [Romano et al. \(2016\)](#) in the general framework of micromorphic continua. Redundancy means that the assumed set of kinematical conditions ensuring rigidity of motion can be substituted with a proper subset of conditions. To see this, we observe that, by virtue Euler's kinematic lemma ([Romano et al., 2016](#), Lemma 1), vanishing of the macro-strain ([Ghayesh and Farajpour, 2019](#), Eq.(27)) implies constancy and skew-symmetry of the displacement gradient. This in turn implies that micro-spin ([Ghayesh and Farajpour, 2019](#), Eq.(31)) is constant and that the microcurvature ([Ghayesh and Farajpour, 2019](#), Eq.(30)) is vanishing. Adoption of the microcurvature tensor as an independent measure of deformation is therefore redundant because its vanishing is already implied by vanishing of the macro-strain. The concept of kinematic redundancy of deformation measures, adopted in the context of generalized continua, was first introduced by [Romano et al. \(2016\)](#) and then acknowledged by the scientific community (see e.g. [Barbagallo et al., 2017](#); [Neff et al., 2017](#); [Sourki and Hosseini, 2017](#)).

## 2. Motivation and outline

The stress-driven nonlocal integral elasticity approach of straight beams by [Romano and Barretta \(2017\)](#), effectively exploited for static, vibration, thermal and buckling problems of nanotechnological interest in ([Oskouie et al., 2018](#); [Apuzzo et al., 2017](#); [Barretta et al., 2018a,b,c, 2019c, 2018d, 2019a,b](#)), is generalized in the present paper to curved nanobeams.

The plan is the following. Kinematics and equilibrium of Bernoulli-Euler curved beams are preliminarily recalled in [Sect.3](#). The stress-driven nonlocal integral formulation of elasticity for curved structures is developed in [Sect.4](#). Assuming that the integral model is governed by the special bi-exponential averaging kernel adopted by [ERINGEN \(1983\)](#), an equivalent differential problem, with homogeneous constitutive boundary conditions, is provided in [Proposition 4.1](#). The stress-driven nonlocal differential problem for straight beams ([Romano and Barretta, 2017, Prop.7.1, p.22](#)) is recovered as a special case by vanishing the geometric curvature of the nano-structural axis line. Equations governing the stress-driven nonlocal elastic equilibrium of curved beams are formulated in [Sect.5](#). Size-dependent elastic behavior of statically determinate and indeterminate curved beams is established and evidenced by illustrations in [Sect.6](#). Results, discussion and closing remarks are summarized in [Sect.7](#).

## 3. Slender curved beams: kinematics and equilibrium

Let us consider a slender curved beam of length  $L$  whose axis is detected by a curve  $\gamma : [0, L] \mapsto V$ , parametrized by the arc length  $s \in [0, L]$ , in a plane  $\pi$  endowed with the linear space of translations  $V$ . The cross-section, assumed to be uniform along  $s$ , is modeled by a two-dimensional domain  $\Omega$ . A geometric sketch of curved beam is depicted in [fig.1](#).

The field of tangent unit vectors to the beam axis is defined by

$$\mathbf{t} := \gamma' \tag{1}$$

where the apex  $(\bullet)'$  is the derivative with respect to  $s$ . Denoting by  $\mathbf{R}$  the linear operator which performs the rotation by  $\pi/2$  counterclockwise in the plane  $\pi$ , we introduce the following field of transversal unit vectors

$$\mathbf{t}_\perp := \mathbf{R}\mathbf{t} \tag{2}$$

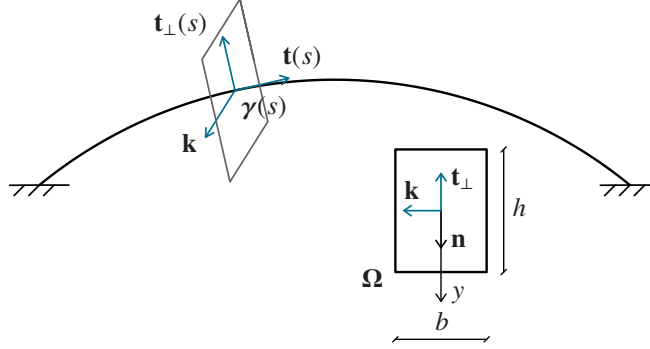


Figure 1: Slender curved beam: a geometric sketch.

and the uniform unit vector field  $\mathbf{k} := \mathbf{t} \times \mathbf{t}_\perp$ , with  $\times$  cross product. According to Bernoulli-Euler's beam theory, cross-sections are clamped to the beam axis  $\gamma$ , and therefore the kinematic model is uniquely described by the translation velocity field  $\mathbf{v} : [0, L] \mapsto V$  of the beam axis. Indeed, in this framework, the angular velocity field  $\omega : [0, L] \mapsto \mathfrak{R}$  of cross-sections is provided by the differential relation

$$\omega = \mathbf{v}' \cdot \mathbf{t}_\perp. \quad (3)$$

The kinematically compatible deformation field  $\mathbf{D}_\mathbf{v}$  associated with the velocity field  $\mathbf{v} : [0, L] \mapsto V$  of the beam axis is given by

$$\mathbf{D}_\mathbf{v} = \begin{vmatrix} \varepsilon_\mathbf{v} \\ \chi_\mathbf{v} \end{vmatrix} = \begin{vmatrix} \mathbf{v}' \cdot \mathbf{t} \\ (\mathbf{v}' \cdot \mathbf{t}_\perp)' \end{vmatrix} \quad (4)$$

in terms of axial strain  $\varepsilon_\mathbf{v} : [0, L] \mapsto \mathfrak{R}$  and flexural curvature  $\chi_\mathbf{v} : [0, L] \mapsto \mathfrak{R}$  scalar fields. The curved beam is subjected to an equilibrated force system  $f$  composed of a distributed vector loading  $\mathbf{p} : [0, L] \mapsto V$  and of boundary concentrated forces  $\mathbf{F}_0 \in V$  and  $\mathbf{F}_L \in V$  and bending couples  $\mathcal{M}_0 \in \mathfrak{R}$  and  $\mathcal{M}_L \in \mathfrak{R}$ . The equilibrated stress  $\boldsymbol{\sigma}$  in a Bernoulli-Euler curved beam is the couple of axial force  $N : [0, L] \mapsto \mathfrak{R}$  and bending moment  $M : [0, L] \mapsto \mathfrak{R}$  fields

$$\boldsymbol{\sigma} = \begin{vmatrix} N \\ M \end{vmatrix} \quad (5)$$

fulfilling the virtual power condition

$$\langle f, \delta \mathbf{v} \rangle = \int_0^L \boldsymbol{\sigma}(s) \cdot \mathbf{D}_{\delta \mathbf{v}}(s) ds, \quad (6)$$

with

$$\begin{aligned} \langle f, \delta \mathbf{v} \rangle := & \int_0^L \mathbf{p}(s) \cdot \delta \mathbf{v}(s) ds + \mathcal{M}_L (\delta \mathbf{v}'(L) \cdot \mathbf{t}_\perp(L)) \\ & + \mathcal{M}_0 (\delta \mathbf{v}'(0) \cdot \mathbf{t}_\perp(0)) + \mathbf{F}_L \cdot \delta \mathbf{v}(L) + \mathbf{F}_0 \cdot \delta \mathbf{v}(0), \end{aligned} \quad (7)$$

virtual power of the force  $f$ , for any virtual velocity field  $\delta \mathbf{v} : [0, L] \mapsto V$  fulfilling homogeneous kinematic boundary conditions. According to Eq.(4), the deformation field  $\mathbf{D}_{\delta \mathbf{v}}$  kinematically compatible with the virtual velocity field  $\delta \mathbf{v}$  is expressed by

$$\mathbf{D}_{\delta \mathbf{v}} = \begin{vmatrix} \varepsilon_{\delta \mathbf{v}} \\ \chi_{\delta \mathbf{v}} \end{vmatrix} = \begin{vmatrix} \delta \mathbf{v}' \cdot \mathbf{t} \\ (\delta \mathbf{v}' \cdot \mathbf{t}_\perp)' \end{vmatrix}. \quad (8)$$

Integrating by parts Eq.(6), applying a standard localization procedure and projecting along the axial  $\mathbf{t}$  and transversal  $\mathbf{t}_\perp$  directions we get the equivalent equilibrium differential problem in  $[0, L]$

$$\begin{cases} N' + T (\mathbf{t}'_\perp \cdot \mathbf{t}) = -\mathbf{p} \cdot \mathbf{t}, \\ T' + N (\mathbf{t}' \cdot \mathbf{t}_\perp) = -\mathbf{p} \cdot \mathbf{t}_\perp, \end{cases} \quad (9)$$

equipped with the boundary conditions at the abscissae  $s = 0$  and  $s = L$

$$\begin{cases} -N(0) \cdot (\delta \mathbf{v} \cdot \mathbf{t})(0) = (\mathbf{F}_0 \cdot \mathbf{t}(0)) \cdot (\delta \mathbf{v} \cdot \mathbf{t})(0), \\ N(L) \cdot (\delta \mathbf{v} \cdot \mathbf{t})(L) = (\mathbf{F}_L \cdot \mathbf{t}(L)) \cdot (\delta \mathbf{v} \cdot \mathbf{t})(L), \\ -M(0) \delta \omega(0) = \mathcal{M}_0 \delta \omega(0), \\ M(L) \delta \omega(L) = \mathcal{M}_L \delta \omega(L), \\ -T(0) \cdot (\delta \mathbf{v} \cdot \mathbf{t}_\perp)(0) = (\mathbf{F}_0 \cdot \mathbf{t}_\perp(0)) \cdot (\delta \mathbf{v} \cdot \mathbf{t}_\perp)(0), \\ T(L) \cdot (\delta \mathbf{v} \cdot \mathbf{t}_\perp)(L) = (\mathbf{F}_L \cdot \mathbf{t}_\perp(L)) \cdot (\delta \mathbf{v} \cdot \mathbf{t}_\perp)(L), \end{cases} \quad (10)$$

with  $T := -M' : [0, L] \mapsto \mathfrak{R}$  shear force interaction field.

In many engineering problems the beam axis is generally regular, so that the vector  $\mathbf{t}'$  is not vanishing and leads to the definition of normal unit vector  $\mathbf{n} := \mathbf{t}'/c$ , with  $c := \|\mathbf{t}'\|$  geometric curvature of the beam axis. The relationship between  $\mathbf{t}_\perp$  and  $\mathbf{n}$  is given by Romano (2002):  $\mathbf{t}_\perp = (\mathbf{t}_\perp \cdot \mathbf{n}) \mathbf{n}$ .

#### 4. Stress-driven nonlocal integral elasticity

Let us preliminarily recall the local elasticity linearized model of Bernoulli-Euler curved beam. Local elastic axial strains  $\varepsilon$  and flexural curvatures  $\chi$  are related to axial forces  $N$  and bending moments  $M$  by Winkler (1858); Baldacci (1983)

$$\begin{cases} \varepsilon(s) = \left[ \frac{1}{EA} [N - cM] \right](s), \\ \chi(s) = \left[ \frac{M}{EJ_r} - \frac{c}{EA} [N - cM] \right](s), \end{cases} \quad (11)$$

with  $E$  Euler-Young modulus,  $A$  cross-sectional area and  $J_r$  is the reduced moment of inertia

$$J_r := \int_{\Omega} y^2 \frac{1}{1 - cy} dA, \quad (12)$$

along the bending axis  $y$  associated with unit normal vector  $\mathbf{n}$ .

Nonlocal effects are described by requiring that elastic axial strains and flexural curvatures are integral convolutions between an averaging kernel  $\phi_l : \mathfrak{R} \mapsto [0; +\infty[$ , described by a nonlocal length parameter  $l \in ]0; +\infty[$ , and the local fields formulated in Eq.(11). The stress-driven nonlocal integral model takes thus the form

$$\begin{cases} \varepsilon(s) = \int_0^L \phi_l(s - \xi) \left[ \frac{1}{EA} [N - cM] \right](\xi) d\xi \\ \chi(s) = \int_0^L \phi_l(s - \xi) \left[ \frac{M}{EJ_r} - \frac{c}{EA} [N - cM] \right](\xi) d\xi \end{cases} \quad (13)$$

Equipping Eq.(13) with the special bi-exponential kernel in (Eringen, 1983)

$$\phi_l(s) = \frac{1}{2l} \exp\left(-\frac{|s|}{l}\right), \quad (14)$$



the stress-driven integral convolutions Eq.(13) can be inverted to give the following constitutive equivalence result, extending thus to curved beams the formulation in (Romano and Barretta, 2017, Prop.7.1, p.22) confined to straight beams. The proof is analogous.

**Proposition 4.1.** *The nonlocal integral formulation for elastic curved beams Eq.(13), equipped with the bi-exponential kernel Eq.(14), is equivalent to the differential problem*

$$\begin{cases} \varepsilon(s) - l^2 (\partial_s^2 \varepsilon)(s) = \left[ \frac{1}{EA} [N - cM] \right] (s), \\ \chi(s) - l^2 (\partial_s^2 \chi)(s) = \left[ \frac{M}{EJ_r} - \frac{c}{EA} [N - cM] \right] (s), \end{cases} \quad (15)$$

with the constitutive boundary conditions (CBC)

$$\begin{cases} \partial_s \varepsilon(0) = \frac{1}{l} \varepsilon(0), \\ \partial_s \varepsilon(L) = -\frac{1}{l} \varepsilon(L), \\ \partial_s \chi(0) = \frac{1}{l} \chi(0), \\ \partial_s \chi(L) = -\frac{1}{l} \chi(L). \end{cases} \quad (16)$$

## 5. Stress-driven nonlocal elastic equilibrium of curved beams

The elastostatic problem of a Bernoulli-Euler curved beam is formulated in terms of displacement field  $\mathbf{u} : [0, L] \mapsto V$  of the structural axis.

In the realm of the geometrically linearized theory, the kinematic relation Eq.(4) holds true, so that the deformation field  $\mathbf{D}_{\mathbf{u}}$  of the curved nanobeam, associated with the displacement field  $\mathbf{u} : [0, L] \mapsto V$ , writes as

$$\mathbf{D}_{\mathbf{u}} = \begin{vmatrix} \varepsilon_{\mathbf{u}} \\ \chi_{\mathbf{u}} \end{vmatrix} = \begin{vmatrix} \mathbf{u}' \cdot \mathbf{t} \\ (\mathbf{u}' \cdot \mathbf{t}_{\perp})' \end{vmatrix} \quad (17)$$

in terms of linearized axial strain  $\varepsilon_{\mathbf{u}} : [0, L] \mapsto \mathfrak{R}$  and linearized flexural curvature  $\chi_{\mathbf{u}} : [0, L] \mapsto \mathfrak{R}$  scalar fields.

Resorting to Eq.(3), the field of rotations  $\varphi : [0, L] \mapsto \mathfrak{R}$  of cross-sections is obtained by integrating Eq.(17)<sub>2</sub>

$$\varphi(s) = (\mathbf{u}' \cdot \mathbf{t}_\perp)(s) = \varphi(0) + \int_0^s \chi_{\mathbf{u}}(\xi) d\xi. \quad (18)$$

To analytically establish the expression of the vector displacement field, let us preliminarily consider the additive decomposition

$$\mathbf{u}' = (\mathbf{u}' \cdot \mathbf{t}) \mathbf{t} + (\mathbf{u}' \cdot \mathbf{t}_\perp) \mathbf{t}_\perp = \varepsilon_{\mathbf{u}} \mathbf{t} + \varphi \mathbf{t}_\perp, \quad (19)$$

where Eqs.(17) and (18) are enforced.

The sought displacement field of the curved nanobeam is obtained by integrating Eq.(19)

$$\mathbf{u}(s) = \mathbf{u}(0) + \int_0^s \mathbf{u}' d\xi = \mathbf{u}(0) + \int_0^s [\varepsilon_{\mathbf{u}}(\xi) \mathbf{t}(\xi) + \varphi(\xi) \mathbf{t}_\perp(\xi)] d\xi. \quad (20)$$

The unknown integration constants  $\varphi(0) \in \mathfrak{R}$  and  $\mathbf{u}(0) \in V$  are univocally evaluated by prescribing the essential kinematic boundary conditions at hand. In all the case-studies presented in the next section, the total deformations  $\{\varepsilon_{\mathbf{u}}, \chi_{\mathbf{u}}\}$  are assumed to be coincident with the elastic deformation fields  $\{\varepsilon, \chi\}$  provided by the stress-driven nonlocal integral convolutions Eq.(13).

## 6. Case-studies

The developed stress-driven methodology is illustrated by investigating the nonlocal behaviour of four static schemes of nanotechnological interest. The nanobeam axis is assumed to be a circle arc of radius  $r = 10$  [nm], so that length and curvature are given by  $L = \pi/(2c)$  and  $c = 1/r$ , respectively. The cross-section  $\Omega$  is a rectangle of base  $b = 1$  [nm] and height  $h = 2$  [nm]. The reduced moment of inertia is evaluated by Eq.(12)

$$J_r = \int_{-b/2}^{+b/2} \int_{-h/2}^{+h/2} \frac{r y^2}{r - y} dy dx \quad (21)$$

The nanobeam is assumed to be made of silicon carbide, with Euler-Young modulus  $E = 427$  [GPa].

In the illustrations below, the following dimensionless nonlocal parameter

$$\lambda = \frac{l}{L}, \quad (22)$$

with  $l$  characteristic length parameter and  $L$  nanobeam length, is adopted.

The solution procedure of the stress-driven nonlocal integral nanostructural problem, formulated in Sect.5, consists of three steps:

1. **Step 1.** Solution of the differential static problem Eqs.(9) and (10). The interaction fields: axial force  $N$ , shear force  $T$  and bending moment  $M$  are expressed in terms of  $n$  integration constants, with  $n$  standing for redundancy degree. For statically determinate beams we have that  $n = 0$  and the stress fields  $N, T, M$  are univocally determined by equilibrium requirements.
2. **Step 2.** Evaluation of axial strain  $\varepsilon$  and bending curvature  $\chi$  by making recourse to the stress-driven integral convolutions Eq.(13) or by solving the differential problem Eq.(15) equipped with the nonlocal boundary conditions Eq.(16), based on the constitutive equivalency established in Prop.4.1.
3. **Step 3.** Prescription of  $3 + n$  essential kinematic boundary conditions and detection of the curved nanobeam nonlocal displacement  $\mathbf{u}$  Eq.(20).

The size-dependent responses of the following four static schemes are studied.

1. **Case 1.** Cantilever curved nanobeam subjected to a uniformly distributed vertical load  $q = 0.1$  [nN]/[nm] directed upwards. The clamp is placed at the abscissa  $s = 0$ , see Fig.2. The essential kinematic boundary conditions are

$$\mathbf{u}(0) = \mathbf{o} \in V, \quad \varphi(0) = 0 \in \mathfrak{R}. \quad (23)$$

The natural static boundary conditions Eq.(10) take thus the form

$$\begin{cases} N(L) & = 0 \in \mathfrak{R}, \\ T(L) & = 0 \in \mathfrak{R}, \\ M(L) & = 0 \in \mathfrak{R}. \end{cases} \quad (24)$$

The structural redundancy degree  $n$  is vanishing and therefore the static problem, recalled at step 1 above, provides the equilibrated axial force  $N$ , shear force  $T$  and bending moment  $M$ , whose graphic representations are reported in Figs.3, 4, 5, respectively. A schematic sketch of the bending axial vector  $M\mathbf{k}$  and of the rotated vector  $\mathbf{R}M\mathbf{k}$  is given in Fig.6. The nonlocal displacement field  $\mathbf{u}$  is got by applying the steps 1 and 2 of the solution strategy above. Plots of the deformed beam axis is provided in Fig.7 for increasing nonlocal parameter  $\lambda$ . Both the deformed and undeformed beam axis are curved lines obtained by parameterizations in terms of the arch length  $s$  and plotted in a Cartesian plane  $x$  [nm],  $y$  [nm]. Note that the classical local solution of elasticity is obtained as the nonlocal parameter tends to zero ( $\lambda = 0^+$ ).

2. **Case 2.** Curved nanobeam with slider and roller supports subjected to a force  $F = 1$  [nN] directed upwards, concentrated at the abscissa  $s = 0$ , shown in Fig.8. The essential kinematic boundary conditions are

$$\mathbf{u}(0) \cdot \mathbf{t}(0) = 0 \in \mathfrak{R}, \quad \varphi(0) = 0 \in \mathfrak{R}, \quad \mathbf{u}(L) \cdot \mathbf{t}(L) = 0 \in \mathfrak{R}. \quad (25)$$

The natural static boundary conditions Eq.(10) take thus the form

$$\begin{cases} T(0) &= -F \in \mathfrak{R}, \\ T(L) &= 0 \in \mathfrak{R}, \\ M(L) &= 0 \in \mathfrak{R}. \end{cases} \quad (26)$$

The nanostructure is statically determinate, so that the redundancy degree  $n$  is vanishing. The solution method, applied to case 1, provides scalar interactions  $N$ ,  $T$ ,  $M$  and vector nonlocal displacements  $\mathbf{u}$ . Graphic outputs are respectively presented in Figs.9, 10, 11 and 12.

3. **Case 3.** Curved nanobeam with slider and clamp supports subjected to a force  $F = 10$  [nN] directed upwards, concentrated at  $s = 0$ , as shown in Fig.13. The essential kinematic boundary conditions are

$$\mathbf{u}(0) \cdot \mathbf{t}(0) = 0 \in \mathfrak{R}, \quad \varphi(0) = 0 \in \mathfrak{R}, \quad \mathbf{u}(L) = 0 \in V, \quad \varphi(L) = 0 \in \mathfrak{R}. \quad (27)$$

The natural static boundary conditions Eq.(10) take thus the form

$$T(0) = -F \in \mathfrak{R}. \quad (28)$$

The nanostructure is statically indeterminate with redundancy degree  $n = 2$ , so that 3+2 essential and 1 natural boundary scalar conditions have to be enforced. The closure of the nonlocal structural problem is therefore guaranteed and the axial force  $N$ , shear force  $T$ , bending moment  $M$  solution fields, associated with the scale parameter  $\lambda = 0.5$ , are depicted in Figs.14, 15, 16. The nonlocal displacement solution field  $\mathbf{u}$  is plotted in Fig.17 for increasing scale parameter  $\lambda$ .

4. **Case 4.** Doubly clamped curved nanobeam under a uniformly distributed vertical load  $q = 5$  [nN]/[nm] directed upwards, see Fig.18. The nanostructure is statically indeterminate with redundancy degree  $n = 3$ , so that the boundary conditions to be imposed are all of kinematic type ( $2 + 1 + 2 + 1 = 6$  scalar prescriptions)

$$\mathbf{u}(0) = 0 \in V, \quad \varphi(0) = 0 \in \mathfrak{R}, \quad \mathbf{u}(L) = 0 \in V, \quad \varphi(L) = 0 \in \mathfrak{R}. \quad (29)$$

No natural static boundary conditions have to be enforced. The elastostatic problem is solved to detect the static and kinematic nonlocal fields  $\{N, T, M\}$ ,  $\mathbf{u}$  in terms of the scale parameter  $\lambda$ . The static outcomes  $\{N, T, M\}$ , corresponding to  $\lambda = 0.5$ , are illustrated in Fig.19, 20, 21, while the nonlocal displacement vector field  $\mathbf{u}$  is depicted in Fig.22 for increasing scale parameter  $\lambda$ .

## 7. Results, discussion and closing remarks

The stress-driven nonlocal integral mechanics of straight elastic beams conceived in (Romano and Barretta, 2017) has been generalized in the present research to curved nanobeams, which are the principal structural elements of new-generation Micro- and Nano-Electro-Mechanical Systems (M/NEMS). The presented integral methodology has been shown to be equivalent to a convenient set of ordinary differential equations, equipped with non-standard nonlocal boundary conditions, generalizing thus to curved nanobeams the constitutive equivalency proposition 7.1 in (Romano and Barretta, 2017). The complex nonlocal elastic equilibrium equations governing the structural problems of engineering interest have been therefore analytically simplified by transforming integral convolutions into equivalent differential conditions.

Unlike strain-driven nonlocal integral and kinematically redundant couple stress models, the stress-driven nonlocal integral formulation of curved elastic nanostructures has been shown to lead to mathematically well-posed problems. An effective solution procedure has been illustrated and implemented by Wolfram's software Mathematica for a variety of nano-engineered structures exploited as sensors and actuators in M/NEMS applications.

In agreement with the experimental results collected in the paper by [Abazari et al. \(2015\)](#) exhibited by a wide range of advanced materials and small-scale devices, a stiffening nano-mechanical behaviour has been predicted by the stress-driven approach in all case-studies for increasing nonlocal parameter. The *smaller-is-stiffer* phenomenon, also predicted in the recent research by [Fuschi et al. \(2019\)](#), seems to be a peculiar property in Nano-Engineering.

### Acknowledgements

The financial support of the Italian Ministry for University and Research (P.R.I.N. National Grant 2017, Project code 2017J4EAYB; University of Naples Federico II Research Unit) is gratefully acknowledged.

### References

- Abazari, A.M., Safavi, S.M., Rezazadeh, G., Villanueva, L.G. (2015). Modelling the Size Effects on the Mechanical Properties of Micro/Nano Structures. *Sensors*, 15, 28543-28562.
- Alfosail F.K., Hajjaj A.Z., Younis M.I. (2019). Theoretical and Experimental Investigation of Two-to-One Internal Resonance in MEMS Arch Resonators. *Journal of Computational and Nonlinear Dynamics, Transactions of the ASME*, 14, 011001.
- Apuzzo, A., Barretta, R., Luciano, R., Marotti de Sciarra, F., Penna, R. (2017). Free vibrations of Bernoulli-Euler nano-beams by the stress-driven nonlocal integral model. *Composites Part B*, 123, 105-111.
- Apuzzo, A., Barretta, R., Faghidian, S.A., Luciano, R., Marotti de Sciarra, F. (2018). Free vibrations of elastic beams by modified nonlocal strain gradient theory. *International Journal of Engineering Science*, 133, 99-108.
- Apuzzo, A., Barretta, R., Faghidian, S.A., Luciano, R., Marotti de Sciarra, F. (2019). Nonlocal strain gradient exact solutions for functionally graded inflected nano-beams. *Composites Part B*, 164, 667-674.

- Arefi, M., Bidgoli, E.M.-R., Dimitri, R., Bacciocchi, M., Tornabene, F. (2019). Nonlocal bending analysis of curved nanobeams reinforced by graphene nanoplatelets. *Composites Part B* 166, 1-12.
- Aya, S.A., Tufekci E. (2017). Modeling and analysis of out-of-plane behavior of curved nanobeams based on nonlocal elasticity. *Composites Part B* 119, 184-195.
- Baldacci, R. (1983). *Scienza delle Costruzioni, Volume II*. Torino: UTET.
- Barbagallo, G., Madeo, A., D'Agostino, M.V., Abreu, R., Ghiba, I.-D., Neff, P. (2017). Transparent anisotropy for the relaxed micromorphic model: Macroscopic consistency conditions and long wave length asymptotics. *International Journal of Solids and Structures*, 120, 7-30.
- Barretta, R., Diaco, M., Feo, L., Luciano, R., Marotti de Sciarra, F., Penna, R. (2018a). Stress-driven integral elastic theory for torsion of nano-beams. *Mechanics Research Communications*, 87, 35-41.
- Barretta, R., Canadija, M., Feo, L., Luciano, R., Marotti de Sciarra, F., Penna, R. (2018b). Exact solutions of inflected functionally graded nano-beams in integral elasticity. *Composites Part B*, 142, 273-286.
- Barretta, R., Canadija, M., Luciano, R., Marotti de Sciarra, F. (2018c). Stress-driven modeling of nonlocal thermoelastic behavior of nanobeams. *International Journal of Engineering Science*, 126, 53-67.
- Barretta, R., Luciano, R., Marotti de Sciarra, F., Ruta, G. (2018d). Stress-driven nonlocal integral model for Timoshenko elastic nano-beams. *European Journal of Mechanics - A/Solids*, 72, 275-286.
- Barretta, R., Faghidian, S.A., Marotti de Sciarra, F., (2019a). Stress-driven nonlocal integral elasticity for axisymmetric nano-plates. *International Journal of Engineering Science*, 136, 38-52.
- Barretta, R., Fabbrocino, F., Luciano, R., Marotti de Sciarra, F., Ruta, G. (2019b). Buckling loads of nano-beams in stress-driven nonlocal elasticity. In Press, Doi: <https://doi.org/10.1080/15376494.2018.1501523>
- Barretta, R., Faghidian, S. A., Luciano R. (2019c). Longitudinal vibrations of nano-rods by stress-driven integral elasticity. *Mechanics of Advanced Materials and Structures*, 26(15), 1307-1315.

- Barretta, R., Marotti de Sciarra, F. (2018). Constitutive boundary conditions for nonlocal strain gradient elastic nano-beams. *International Journal of Engineering Science*, 130, 187-198.
- Barretta, R., Marotti de Sciarra, F. (2019). Variational nonlocal gradient elasticity for nano-beams. *International Journal of Engineering Science*, 143, 73-91.
- Challamel, N., Wang, C.M. (2008). The small length scale effect for a non-local cantilever beam: a paradox solved. *Nanotechnology*, 19, 345703.
- Chorsi, M.T., Chorsi, H.T. (2018). Modeling and analysis of MEMS disk resonators. *Microsystem Technologies*, 24(6), 2517-2528.
- Dantas, W.G., Gusso, A. (2018). Analysis of the Chaotic Dynamics of MEMS/NEMS Doubly Clamped Beam Resonators with Two-Sided Electrodes. *International Journal of Bifurcation and Chaos*, 28(10), 1850122.
- Dehrouyeh-Semnani, A.M., Nikkhah-Bahrami, M., Yazdi, M.R.H. (2017a). On nonlinear vibrations of micropipes conveying fluid. *International Journal of Engineering Science*, 117, 20-33.
- Dehrouyeh-Semnani, A.M., Nikkhah-Bahrami, M., Yazdi, M.R.H. (2017b). On nonlinear stability of fluid-conveying imperfect micropipes. *International Journal of Engineering Science*, 120, 254-271.
- Ding, H., Ma, Y., Guan, Y., Ju, B.-F., Xie, J. (2019). Duplex mode tilt measurements based on a MEMS biaxial resonant accelerometer. *Sensors and Actuators, A: Physical*, 296, 222-234.
- Ebrahimi, F., Barati, M.R. (2017). A nonlocal strain gradient refined beam model for buckling analysis of size-dependent shear-deformable curved FG nanobeams. *Composite Structures*, 159, 174-182.
- Ebrahimi, F., Barati, M.R. (2018). Vibration analysis of piezoelectrically actuated curved nanosize FG beams via a nonlocal strain-electric field gradient theory. *Mechanics of Advanced Materials and Structures*, 25(4), 350-359
- Eringen, A.C. (1972). Linear theory of nonlocal elasticity and dispersion of plane waves. *International Journal of Engineering Science*, 10(5), 425-435.



- Eringen, A.C. (1983). On differential equations of nonlocal elasticity and solutions of screw dislocation and surface waves. *Journal of Applied Physics*, 54, 4703.
- Eringen, A.C. (1987). Theory of nonlocal elasticity and some applications. *Res Mechanica*, 21, 313-342.
- Farokhi, H., Ghayesh, M.H., Gholipour, A., Hussain, S. (2017). Motion characteristics of bilayered extensible Timoshenko microbeams. *International Journal of Engineering Science*, 112, 1-17.
- Farokhi, H., Ghayesh, M.H. (2018a). Nonlinear mechanics of electrically actuated microplates. *International Journal of Engineering Science*, 123, 197-213.
- Farokhi, H., Ghayesh, M.H. (2018b). Nonlinear mechanical behaviour of microshells. *International Journal of Engineering Science*, 127, 127-144.
- Farokhi H., Ghayesh M.H., (2018c). Viscoelasticity effects on resonant response of a shear deformable extensible microbeam. *Nonlinear Dynamics* (2017) 87, 391-406.
- Fernández-Sáez, J., Zaera, R., Loya, J.A., Reddy, J.N. (2016) Bending of Euler-Bernoulli beams using Eringen's integral formulation: A paradox resolved. *International Journal of Engineering Science*, 99, 107-116.
- Fernández-Sáez, J., Zaera, R. (2017). Vibrations of Bernoulli-Euler beams using the two-phase nonlocal elasticity theory. *International Journal of Engineering Science*, 119, 232-248.
- Frangi, A., Gobat, G. (2019). Reduced order modelling of the non-linear stiffness in MEMS resonators. *International Journal of Non-Linear Mechanics*, 116, 211-218.
- Fuschi P., Pisano, A.A., Polizzotto C. (2019). Size effects of small-scale beams in bending addressed with a strain-difference based nonlocal elasticity theory. *International Journal of Mechanical Sciences*, 151, 661-671.
- Ganapathi, M., Polit, O. (2017). Dynamic characteristics of curved nanobeams using nonlocal higher-order curved beam theory. *Physica E*, 91, 190-202.

- Ghayesh, M.H., Farokhi, H., (2017a). Nonlinear mechanics of doubly curved shallow microshells. *International Journal of Engineering Science*, 119, 288-304.
- Ghayesh, M.H., Farokhi, H. (2017b). Parametric vibrations of imperfect Timoshenko microbeams. *Microsystem Technologies*, 23, 4917-4929.
- Ghayesh, M.H., Farokhi, H., Gholipour, A., Tavallaeinejad, M. (2018). Non-linear oscillations of functionally graded microplates. *International Journal of Engineering Science*, 122, 56-72.
- Ghayesh, M.H., (2019). Viscoelastic dynamics of axially FG microbeams. *International Journal of Engineering Science*, 135, 75-85.
- Ghayesh, M.H., Farajpour, A. (2019). A review on the mechanics of functionally graded nanoscale and microscale structures. *International Journal of Engineering Science*, 137, 8-36.
- Karami, B., Shahsavari, D., Janghorban, M., Li, L. (2019a). Influence of homogenization schemes on vibration of functionally graded curved microbeams. *Composite Structures*, 216, 67-79.
- Karami, B., Shahsavari, D., Janghorban, M. (2019b). On the dynamics of porous doubly-curved nanoshells. *International Journal of Engineering Science*, 143, 39-55.
- Khaniki, H.B. (2019). On vibrations of FG nanobeams. *International Journal of Engineering Science*, 135, 23-36.
- Khorshidi, M.A. (2018). The material length scale parameter used in couple stress theories is not a material constant. *International Journal of Engineering Science*, 133, 15-25.
- Kurmendra, Kumar, R. (2019). MEMS based cantilever biosensors for cancer detection using potential bio-markers present in VOCs: a survey. *Microsystem Technologies*, 25(9), 3253-3267.
- Kurmendra, Rahul, J., Kumar, R. (2019). Micro-cantilevered MEMS Biosensor for Detection of Malaria Protozoan Parasites. *Journal of Computational Applied Mechanics*, 50(1), 99-107.

- Lekha, C.S.C., Kumar, A.S., Vivek, S., Rasi, U.P.M., Saravanan, K.V., Nandakumar, K., Nair, S.S. (2017). High voltage generation from lead-free magnetoelectric coaxial nanotube arrays and their applications in nano energy harvesters. *Nanotechnology*, 28(5), 055402.
- Lim, C.W., Zhang, G., Reddy J.N. 2015. A higher-order nonlocal elasticity and strain gradient theory and its applications in wave propagation. *Journal of the Mechanics and Physics of Solids*, 78, 298-313.
- Li, C., Yao, L., Chen W., Li, S. (2015). Comments on nonlocal effects in nano-cantilever beams. *International Journal of Engineering Science*, 87, 47-57.
- Neff, P., Madeo, A., Barbagallo, G., D'Agostino, M.V., Abreu, R., Ghiba, I.-D. (2017). Real wave propagation in the isotropic-relaxed micromorphic model. *Proceedings of the Royal Society A: Mathematical, Physical and Engineering Sciences*, 473 (2197), 20160790.
- Nikpourian, A., Ghazavi, M.R., Azizi, S. (2019). Size-dependent secondary resonance of a piezoelectrically laminated bistable MEMS arch resonator. *Composites Part B*, 173,106850
- Oskouie, M. F., Ansari, R., Rouhi, H. (2018). Bending of Euler-Bernoulli nanobeams based on the strain-driven and stress-driven nonlocal integral models: a numerical approach. *Acta Mechanica Sinica*. Doi: 10.1007/s10409-018-0757-0
- Ouakad, H.M., Najar, F. (2019). Nonlinear dynamics of MEMS arches assuming out-of-plane actuation arrangement. *Journal of Vibration and Acoustics, Transactions of the ASME*, 141(4), 041010.
- Ouakad, H.M., Sedighi, H.M. (2019). Static response and free vibration of MEMS arches assuming out-of-plane actuation pattern. *International Journal of Non-Linear Mechanics*, 110, 44-57.
- Peddieon J, Buchanan GR, McNitt RP. (2003). Application of nonlocal continuum models to nanotechnology. *International Journal of Engineering Science*, 41(3-5), 305-312.
- Polit, O., Merzouki, T., Ganapathi, M. (2018). Elastic stability of curved nanobeam based on higher-order shear deformation theory and nonlocal

- analysis by finite element approach. *Finite Elements in Analysis and Design*, 146, 1-15.
- Rezaiee-Pajand, M., Rajabzadeh-Safaei, N. (2018). Nonlocal static analysis of a functionally graded material curved nanobeam. *Mechanics of Advanced Materials and Structures*, 25(7), 539-547.
- Romano, G. (2002). *Scienza delle Costruzioni*, Tomo I. Benevento: Hevelius.
- Romano, G., Barretta, R. (2016). Comment on the paper “Exact solution of Eringen’s nonlocal integral model for bending of Euler-Bernoulli and Timoshenko beams” by Meral Tuna & Mesut Kirca. *International Journal of Engineering Science*, 109, 240-242.
- Romano, G., Barretta, R., Diaco, M. (2016). Micromorphic continua: non-redundant formulations. *Continuum Mechanics and Thermodynamics*, 28, 1659-1670.
- Romano, G., Barretta, R. (2017). Nonlocal elasticity in nanobeams: the stress-driven integral model. *International Journal of Engineering Science*, 115, 14-27.
- Romano, G., Barretta, R., Diaco, M. (2017). On nonlocal integral models for elastic nano-beams. *International Journal of Mechanical Sciences*, 131-132, 490-499.
- Romano, G., Barretta, R., Diaco, M., Marotti de Sciarra, F. (2017). Constitutive boundary conditions and paradoxes in nonlocal elastic nano-beams. *International Journal of Mechanical Sciences*, 121, 151-156.
- Salim, M., Salim, D., Chandran, D., Aljibori, H.S., Kherbeet, A.S. (2018). Review of nano piezoelectric devices in biomedicine applications. *Journal of Intelligent Material Systems and Structures*, 29(10), 2105-2121.
- Sedighi, H.M., Koochi, A., Keivani, M., Abadyan, M. (2017). Measurement: *Journal of the International Measurement Confederation*, 111, 114-121.
- She, G.-L., Yuan, F.-G., Karami, B., Ren, Y.-R., Xiao, W.-S. (2019a). On nonlinear bending behavior of FG porous curved nanotubes. *International Journal of Engineering Science*, 135, 58-74.

- She, G.-L., Ren, Y.-R., Yan, K.-M. (2019b). On snap-buckling of porous FG curved nanobeams. *Acta Astronautica*, 161, 475-484.
- Sieberer, S., McWilliam, S., Popov, A.A. (2019). Nonlinear electrostatic effects in MEMS ring-based rate sensors under shock excitation. *International Journal of Mechanical Sciences*, 157-158, 485-497.
- Sobhy, M., Abazid, M.A. (2019). Dynamic and instability analyses of FG graphene-reinforced sandwich deep curved nanobeams with viscoelastic core under magnetic field effect. *Composites Part B*, 174, 106966.
- Sourki, R., Hosseini, S.A. (2017). Coupling effects of nonlocal and modified couple stress theories incorporating surface energy on analytical transverse vibration of a weakened nanobeam. *European Physical Journal Plus*, 132(4), 184.
- Taati, E. (2018). On buckling and post-buckling behavior of functionally graded micro-beams in thermal environment. *International Journal of Engineering Science*, 128, 63-78.
- Wang, Y., Zhu, X., Dai, H. (2016). Exact solutions for the static bending of Euler-Bernoulli beams using Eringen two-phase local/nonlocal model. *AIP Advances*, 6(8), 085114. Doi:10.1063/1.4961695
- Yang, F, Chong, A, Lam, D.C., Tong, P. (2002). Couple stress based strain gradient theory for elasticity. *International Journal of Solids and Structures*, 39, 2731-2743.
- Wang, Z., Ren, J. (2019). Three-to-one internal resonance in MEMS arch resonators. *Sensors*, 19(8),1888.
- Winkler E., (1858). *Formänderung und Festigkeit gekrümmter Körper, insbesondere der Ringe* *Civilingenieur* 4, 232-246.
- Zhang, P., Qing H., Gao, C. (2019). Theoretical analysis for static bending of circular Euler-Bernoulli beam using local and Eringen's nonlocal integral mixed model. *ZAMM*. In Press. <https://doi.org/10.1002/zamm.201800329>
- Zhu, X.W., Wang, Y.B., Dai, H.H. (2017). Buckling analysis of Euler-Bernoulli beams using Eringen's two-phase nonlocal model. *International Journal of Engineering Science*, 116, 130-140.

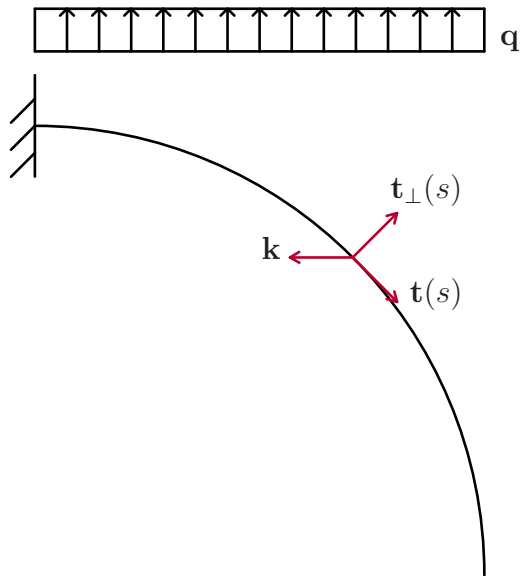


Figure 2: Cantilever curved nanobeam.

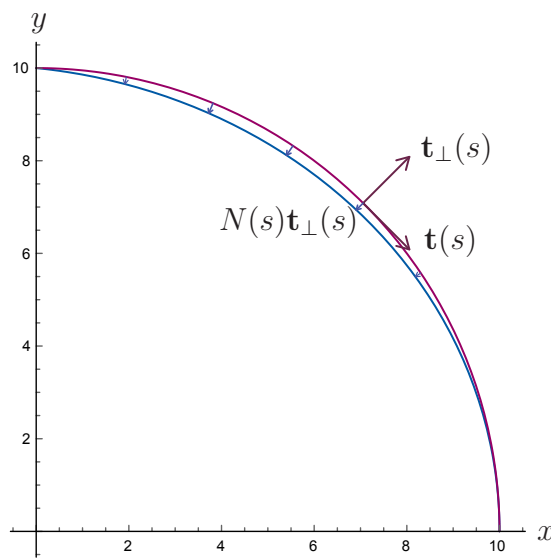


Figure 3: Cantilever curved nanobeam: plot of the vector field  $N\mathbf{t}_\perp$ .

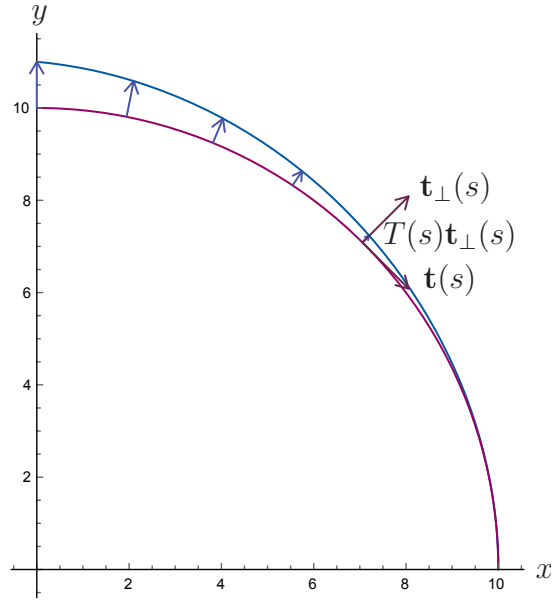


Figure 4: Cantilever curved nanobeam: plot of the vector field  $T\mathbf{t}_\perp$ .

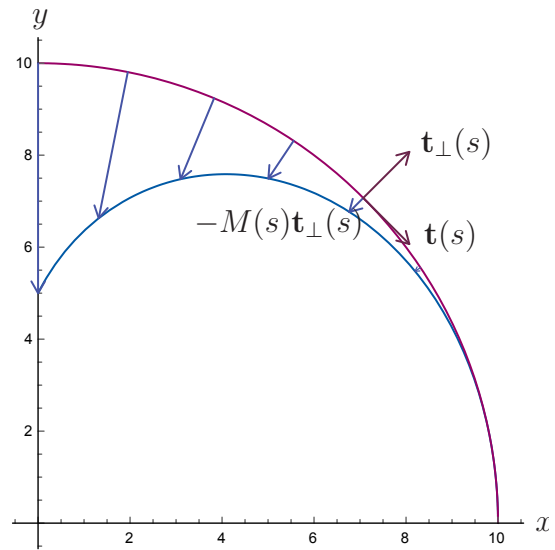


Figure 5: Cantilever curved nanobeam: plot of the vector field  $\mathbf{R}(\mathbf{M}\mathbf{k}) = -M\mathbf{t}_\perp$ .

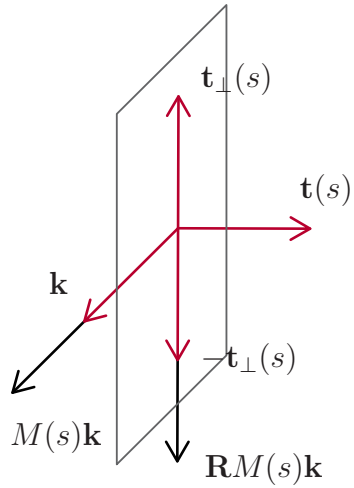


Figure 6: Cross section at abscissa  $s$  with the local triad and the vectors  $M\mathbf{k}$  and  $\mathbf{R}M\mathbf{k}$ .

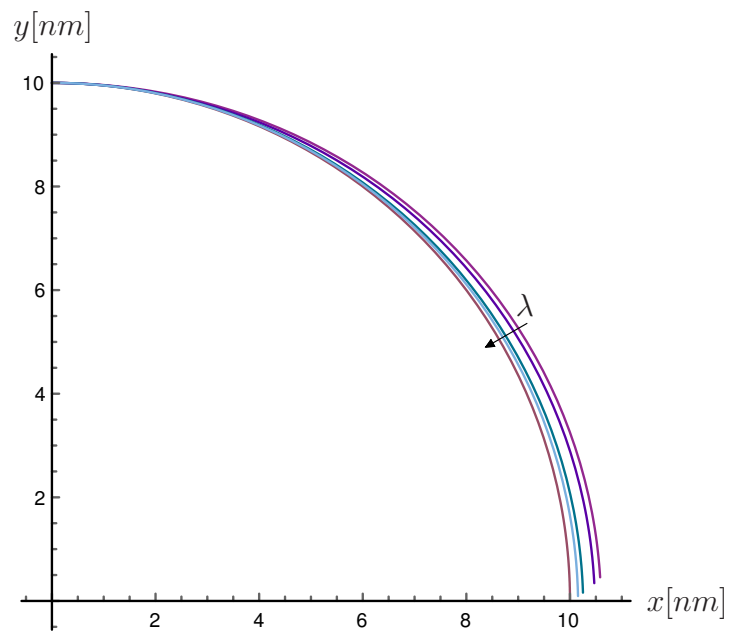


Figure 7: Cantilever curved nanobeam: deflection of the beam axis for  $\lambda \in \{0; 0.1; 0.5; 1\}$ .



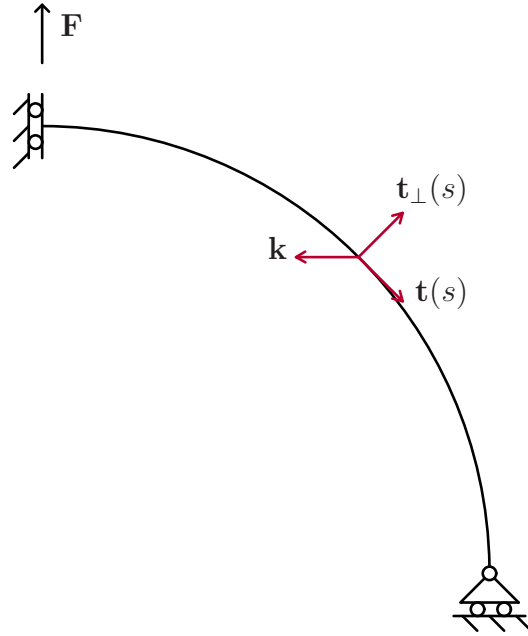


Figure 8: Curved nanobeam with slider and roller supports.

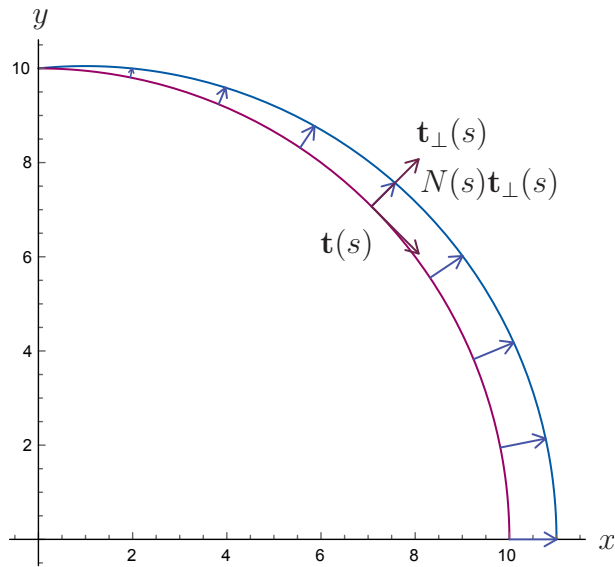


Figure 9: Curved nanobeam with slider and roller supports: plot of the vector field  $N\mathbf{t}_\perp$ .

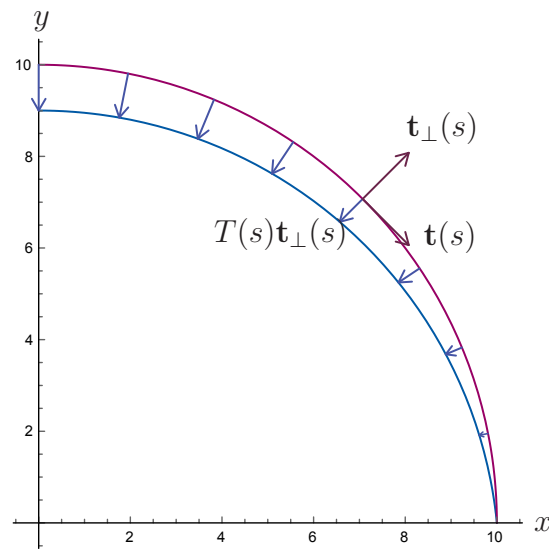


Figure 10: Curved nanobeam with slider and roller supports: plot of the vector field  $T\mathbf{t}_\perp$ .

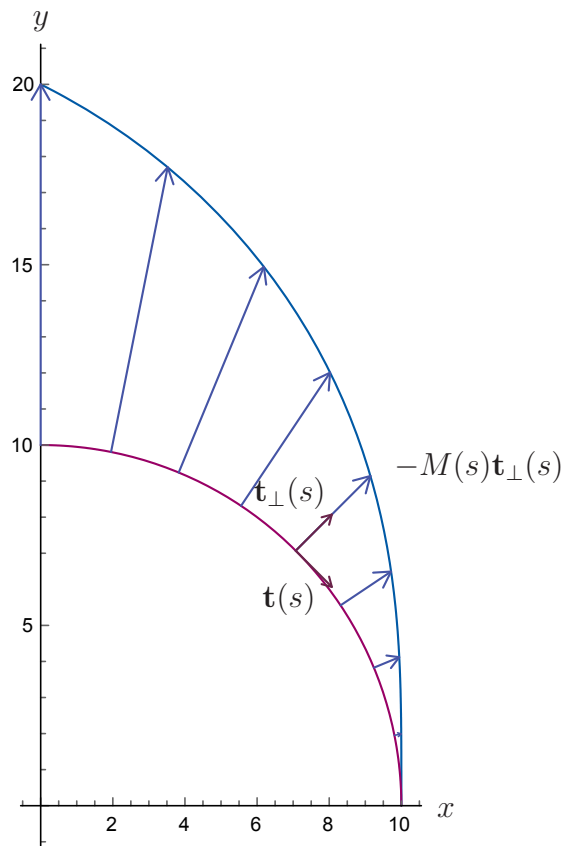


Figure 11: Curved nanobeam with slider and roller supports: plot of the vector field  $\mathbf{R}(\mathbf{M}\mathbf{k}) = -M\mathbf{t}_\perp$ .

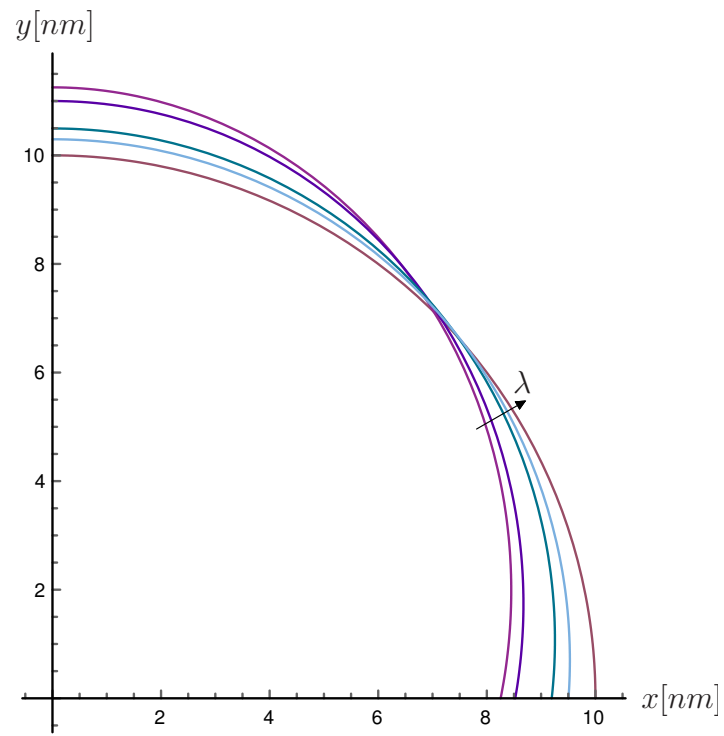


Figure 12: Curved nanobeam with slider and roller supports: deflection of the beam axis for  $\lambda \in \{0; 0.1; 0.5; 1\}$ .

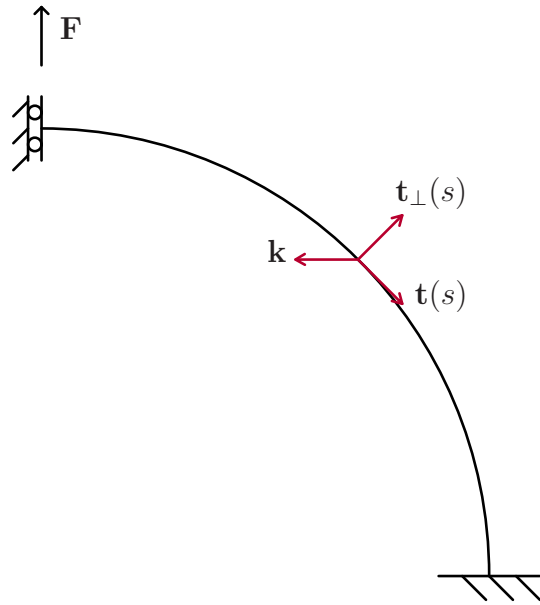


Figure 13: Curved nanobeam with slider and clamp supports.

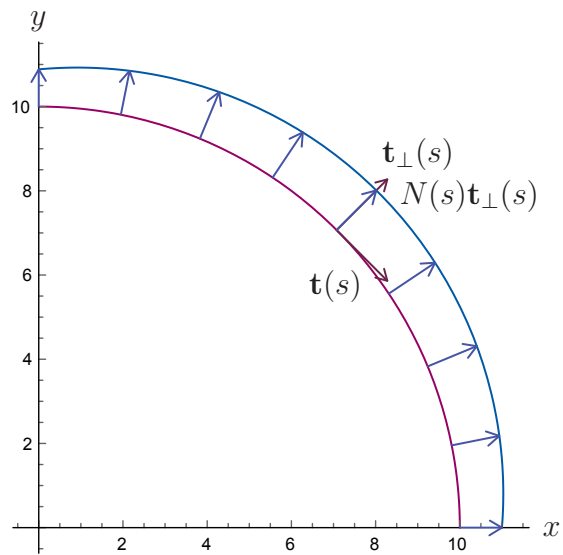


Figure 14: Curved nanobeam with slider and clamp supports: plot of the vector field  $N\mathbf{t}_\perp$ .

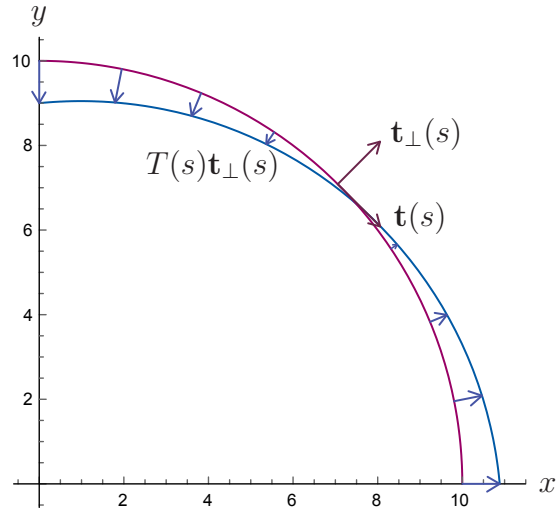


Figure 15: Curved nanobeam with slider and clamp supports: plot of the vector field  $T\mathbf{t}_\perp$ .

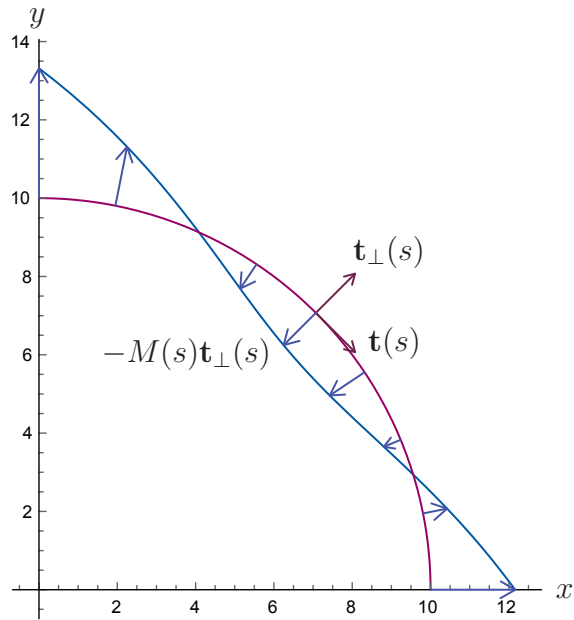


Figure 16: Curved nanobeam with slider and clamp supports: plot of the vector field  $\mathbf{R}(\mathbf{Mk}) = -M\mathbf{t}_\perp$ .

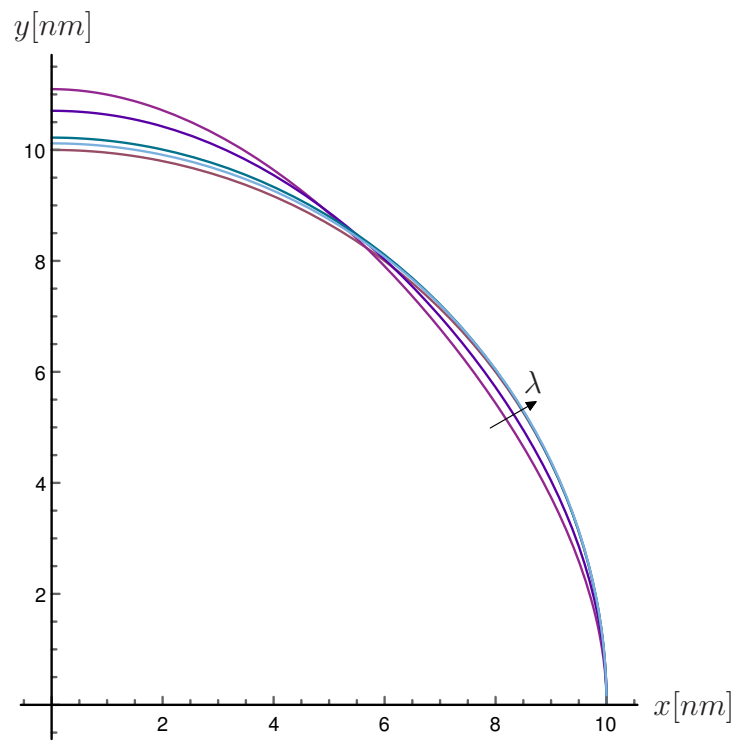


Figure 17: Curved nanobeam with slider and clamp supports: deflection of the beam axis for  $\lambda \in \{0; 0.1; 0.5; 1\}$ .

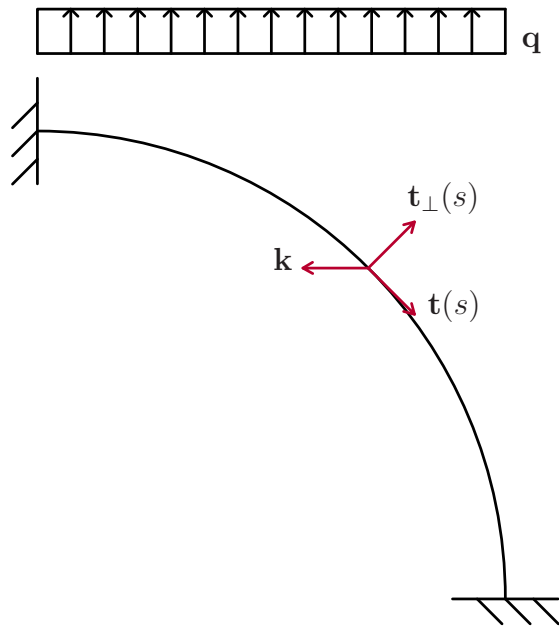


Figure 18: Doubly clamped curved nanobeam



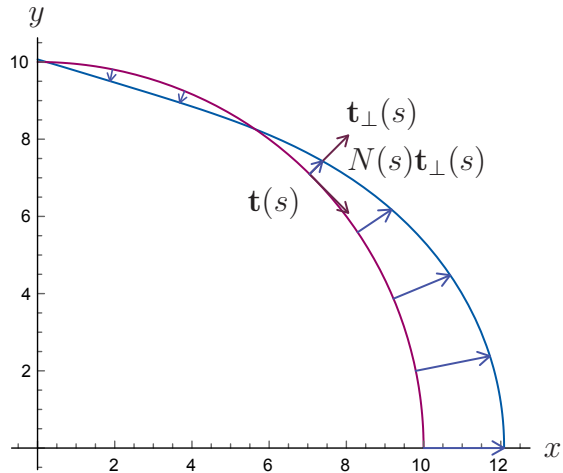


Figure 19: Doubly clamped curved nanobeam: plot of the vector field  $N\mathbf{t}_\perp$ .

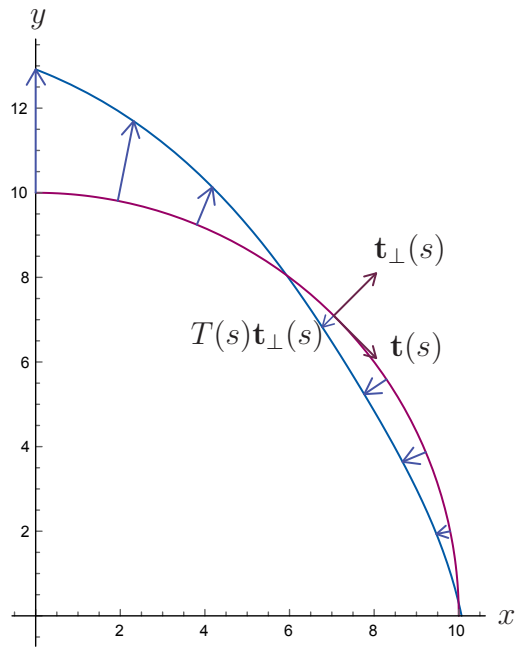


Figure 20: Doubly clamped curved nanobeam: plot of the vector field  $T\mathbf{t}_\perp$ .

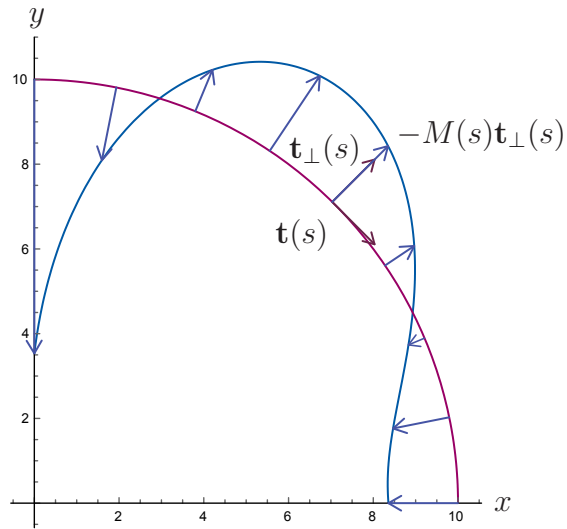


Figure 21: Doubly clamped curved nanobeam: plot of the vector field  $\mathbf{R}(M\mathbf{k}) = -Mt_{\perp}$ .

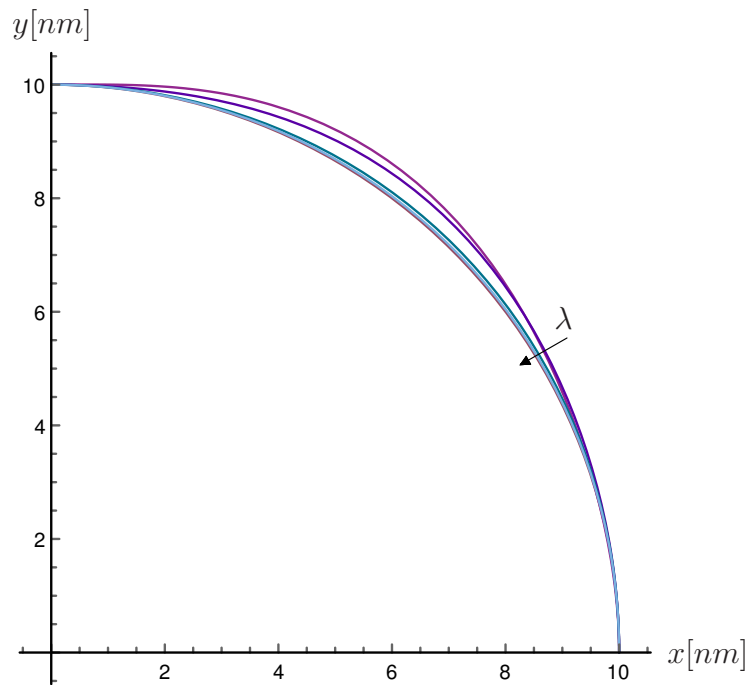


Figure 22: Doubly clamped curved nanobeam: deflection of the beam axis for  $\lambda \in \{0; 0.1; 0.5; 1\}$ .